

The effect of venting on cookoff of a melt-castable explosive (Comp-B)

Michael L. Hobbs^{*†} and Michael J. Kaneshige^{**}

Sandia National Laboratories, Albuquerque, NM 87185 USA

^{*}Engineering Sciences Center

^{**}Energetics Components Center,

[†]Corresponding author : mlhobbs@sandia.gov

Phone : +010-1-505-844-5988

Received : November 12, 2014 Accepted : February 18, 2015

Abstract

Occasionally, our well-controlled cookoff experiments with Comp-B give anomalous results when venting conditions are changed. For example, a vented experiment may take longer to ignite than a sealed experiment. In the current work, we show the effect of venting on thermal ignition of Comp-B. We use Sandia's Instrumented Thermal Ignition (SITI) experiment with various headspace volumes in both vented and sealed geometries to study ignition of Comp-B. In some of these experiments, we have used a boroscope to observe Comp-B as it melts and reacts. We propose that the mechanism for ignition involves TNT melting, dissolution of RDX, and complex bubbly liquid flow. High pressure inhibits bubble formation and flow is significantly reduced. At low pressure, a vigorous dispersed bubble flow was observed.

Keywords : Comp-B, cookoff, sealed, vented, two-phase reactive flow

1. Introduction

The melt castable explosive Composition B (Comp-B) is nominally composed of 63/36/1 RDX/TNT/wax by weight and has been used in various warheads and demolition charges. Comp-B does not always pass slow and fast cookoff insensitive munitions tests¹⁾. Consequently, the response of Comp-B to accidental fires is important for safety considerations. Melting TNT, RDX dissolution in hot liquid TNT, decomposition gas bubble formation, and bubbly flow complicate the cookoff response of Comp-B.

Prior modeling has focused on thermal and chemistry effects with little regard to flow. For example, Zerkle²⁾ presented a decomposition model of Comp-B by combining separate TNT and RDX mechanisms. The predicted ignition times for Comp-B were higher than the measured ignition times. Zerkle suggested that dissolution of RDX into molten TNT effectively reduces the activation barrier, causing the mixture to ignite sooner.

More recently, Hobbs *et al.*³⁾ predicted cookoff of Comp-B using a single-phase flow model by assuming the Comp-B, gas products, and condensed products move at the same velocity. An effective capacitance method was used

to model the TNT phase change and RDX dissolution. Predicted ignition times for Sandia's Instrumented Thermal Ignition (SITI) experiments matched measured ignition times for confined experiments, but predictions for vented experiments were not adequate. McClelland *et al.*⁴⁾ also modeled cookoff of Comp-B in the One-Dimensional Time-to-eXplosion (ODTX) experiment⁵⁾ with limited success.

In previous work,³⁾ we found that flow effects were different from our Boussinesq flow predictions. We have investigated this model and data discrepancy using a camera (boroscope) to take in situ videos of Comp-B decomposition within our SITI experiments. We have formulated a simple Comp-B model based on these observations to describe cookoff of Comp-B in both sealed and vented experiments.

2. Experimental

The purpose of our experiments is to determine the effect of 1) pressure and 2) venting on decomposition of Comp-B leading to cookoff. In the current paper, we have used our own experiments (SITI) in several configurations to investigate both venting effects and pressure effects.

For the venting effects, we allowed the decomposition gases to leave the confining aluminum apparatus. For the pressure effect we changed the free volume or headspace within the confining apparatus to investigate decomposition at different pressure levels. To validate our results, we have also looked at sealed experiments (ODTX) in a different geometry performed by others at a different laboratory.

2.1 SITI Experiments

Figure 1. A shows a schematic of a SITI experiment with a large headspace volume and a camera (boroscope). The thermocouple junctions are located in the center of the 0.0254 m diameter by 0.0254 m tall cylinder of Comp-B

as shown in Figure 1. B. Figure 1. C shows the nominal SITI schematic with a smaller headspace designed to accommodate thermal expansion of the Comp-B. The smaller headspace SITI is simulated in the current work with the finite element mesh shown in Figure 1. D. The outside temperature of the confining aluminum cylinders is typically ramped from room temperature to a set point temperature in 10 minutes. Pressure is measured with a tube connected to a pressure transducer.

2.2 ODTX Experiments

A 0.0127 m diameter sphere of Comp-B is confined between two 0.0762 m diameter aluminum cylinders with a hemisphere machined into both cylinders to

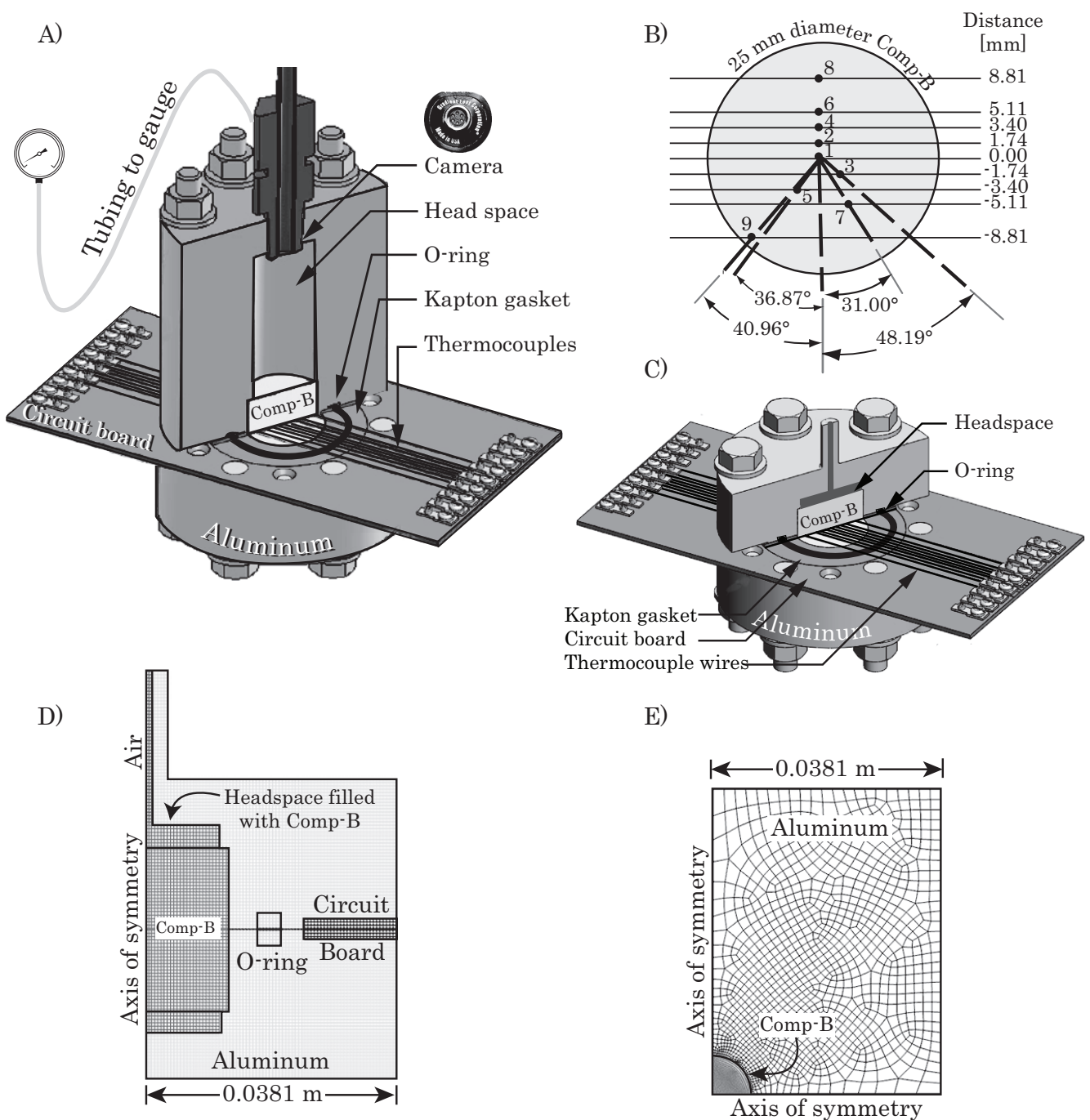


Figure 1 A) SITI with large headspace to accommodate a boroscope, B) Cross-section of Comp-B in SITI apparatus showing thermocouple locations, C) SITI with small headspace, D) SITI mesh, and E) ODTX mesh.

accommodate the explosive. A copper ring is plastically deformed in a groove that is machined into the anvils near the explosive edge. The cylinders are heated to a prescribed temperature, giving a constant temperature boundary condition for the one-dimensional experiment. McGuire and Tarver⁵⁾ give more detail regarding the ODTX experiments. The mesh used to simulate the ODTX experiments is shown in Figure 1. E. The axes of symmetry labeled in Figure 1. D and 1. E are used to simplify the computational models.

2.3 Results

Figure 2 shows a comparison of temperatures and pressures measured for two sealed SITI experiments: 1) experiment #372 with a small headspace volume and 2) experiment #373 with a large headspace volume. The headspace and tubing volumes for #372 and #373 are $3.02 \times 10^{-6} \text{ m}^3$ and $20.1 \times 10^{-6} \text{ m}^3$, respectively. For experiment #372 the top headspace is similar to the bottom headspace. However, for experiment #373, the top headspace is significantly larger than the bottom headspace. In Figure 2, the temperatures are plotted as solid lines, the pressures are plotted as dashed lines, and the boundary temperature is plotted as a dash dot line. All nine thermocouple locations, which were shown in Figure 1. B, are plotted in Figure 2. A, but for clarity only the center temperatures measured with thermocouple #1 and the aluminum boundary temperatures are plotted in Figure 2. B. The TNT melt, which starts about 354 K, is annotated in Figure 2. A.

Figures 2. A and 2. B both show that the center temperature reached the outside boundary temperature more quickly in experiment #373 with the larger headspace of 20 cm^3 than in experiment #372 with the smaller headspace of 3 cm^3 . The pressure in experiment #373 is also less than the pressure in experiment #372 due to the larger headspace. We hypothesize that the lower pressure in experiment #373 was more favorable for bubble formation leading to bubbly flow with increased

heat transfer and a correspondingly longer ignition time. The ignition time for #372 and #373 was 1730 s and 1830 s, respectively.

Figure 3 shows a comparison of temperatures for two SITI experiments with large headspace volumes: 1) vented experiment #370 and 2) sealed experiment #373). Figure 3 also shows boroscope pictures from #370 and #373. The larger white spots in these images may be caused by reflected light from the boroscope. The measured pressure from #373 is also plotted in Figure 3. A.

Figure 3. A shows that the temperature increases to the temperature of the aluminum container more quickly for vented experiment #370 than for sealed experiment #373. Similar to the observation made with Figure 2, we postulate that the faster rise in temperature is due to better mixing for the lower pressure vented experiment. The hypothesis is supported by the boroscope images in Figure 3. C and D, which show less bubble formation in the sealed #373 than in the vented #370.

Observations from these new SITI experiment are that 1) increased pressure diminishes bubble formation and mixing, 2) pressure has a *small effect* on the ignition chemistry for confined experiments, and 3) venting has a *large effect* on convective heat transfer and subsequent ignition times. Pressure suppresses the two-phase flow while venting causes rapid movement with significant bubble formation.

3. Engineering Model

Pressure has a *minor effect on decomposition chemistry* as shown in Figure 2 but plays a *major role in flow behavior* as shown in Figure 3. Such results indicate that flow is 1) subdued in small-scale *sealed* experiments such as the ODTX and SITI experiments and 2) enhanced by rapid bubble formation in the vented or SITI experiments with significant headspace. These observations suggest a few model simplifications: 1) sealed cases can be run assuming no flow, and 2) vented cases can be run with enhanced heat transfer approaching a zero-dimensional, well-stirred

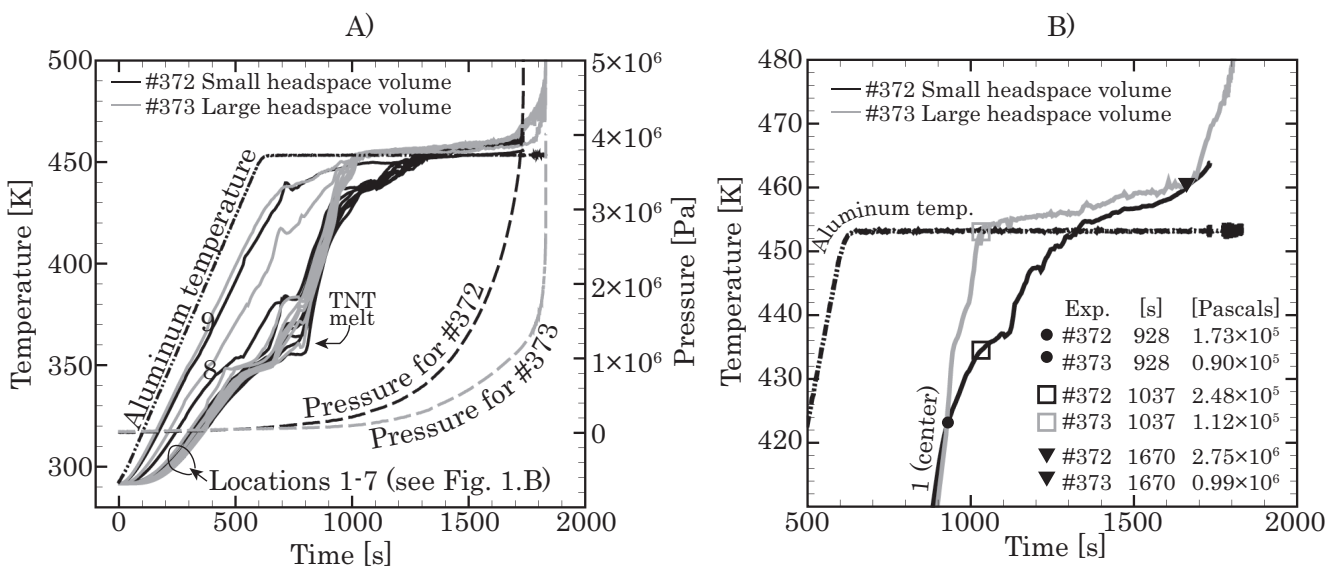


Figure 2 Detailed temperature and pressure plots for #372 and #373. A) Plot showing all measured temperatures B) plots showing center and boundary temperatures.

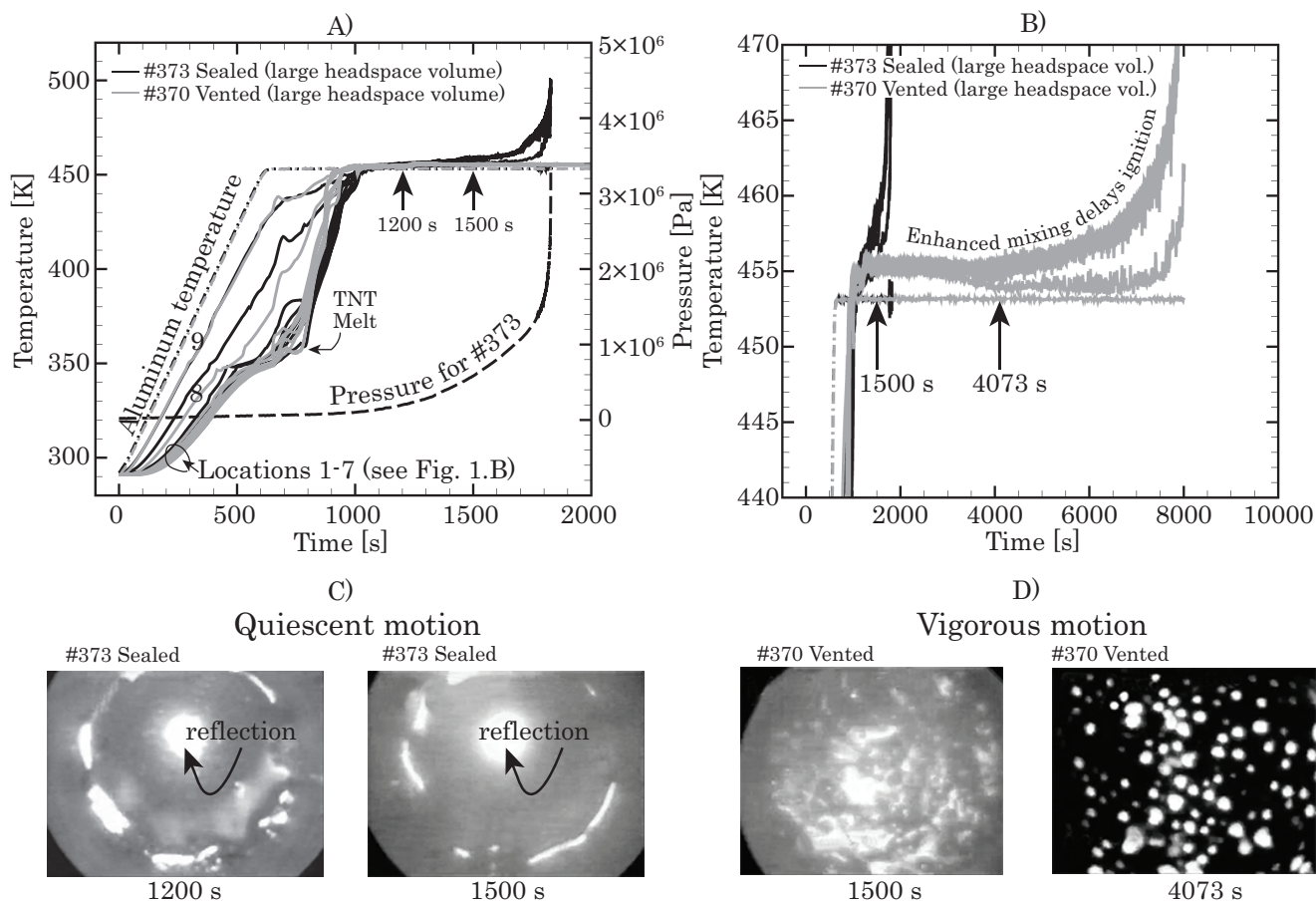


Figure 3 Temperature, pressure and boroscope images from #370 and #373. Plots in A and B use different axis. Boroscope images are from C) #373 and D) #370.

mixing model.

We model thermal ignition of Comp-B by solving the conductive energy equation using a volumetric source for chemical reactions.

$$\rho_b C_b \frac{\partial T}{\partial t} = \nabla \cdot (k \nabla T) + r h_{rxn} M_w. \quad (1)$$

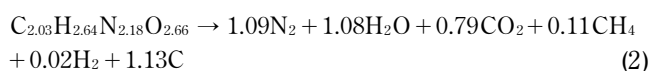
In Equation (1), ρ_b , C_b , T , t , k , r , h_{rxn} , and M_w represent the bulk density, bulk specific heat, temperature, time, thermal conductivity, reaction rate, reaction enthalpy, and molecular weight, respectively. The density of Comp-B in the SITI reactions was $1707 \text{ kg} \cdot \text{m}^{-3}$. The pellets were assumed to thermally expand and fill the gap shown in Figure 1. C giving an average bulk density of $1650 \text{ kg} \cdot \text{m}^{-3}$. The density of the Comp-B in the ODTX experiments was $1630 \text{ kg} \cdot \text{m}^{-3}$.

The baseline specific heat was taken from McGuire and Tarver⁵⁾ by taking a weighted average of the RDX and TNT specific heats, $C_p [\text{J} \cdot \text{kg}^{-1} \text{K}^{-1}] = 2.1538 \times T [\text{K}] + 413.15$. An effective capacitance method was used to account for the latent enthalpy for the TNT ($32 \text{ J} \cdot \text{g}_{\text{Comp-B}}^{-1}$) and RDX ($89 \text{ J} \cdot \text{g}_{\text{Comp-B}}^{-1}$).³⁾ The latent enthalpy for the TNT was distributed with a triangular distribution between 346.15 K (73°C) and 362.15 K (89°C) with the effective capacitance being $5240 \text{ J} \cdot \text{kg}^{-1} \text{K}^{-1}$ at 354.15 K (81°C), the TNT melting point. The spread of the distribution for the TNT melt was chosen to best match SITI data. The latent enthalpy for the RDX was

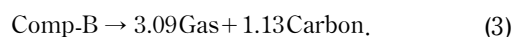
distributed with a triangular distribution between 470.65 K (197.5°C) and $(480.65 \text{ K}) 207.5^\circ\text{C}$ with the effective capacitance being $19,200 \text{ J} \cdot \text{kg}^{-1} \text{K}^{-1}$ at 475.65 (202.5°C), the RDX melting point. The spread for the RDX melt was chosen based on DSC data.

The thermal conductivity was assumed to be $0.20 \text{ W} \cdot \text{m}^{-1} \text{K}^{-1}$ for temperatures less than 364.15 K (73°C), $0.15 \text{ W} \cdot \text{m}^{-1} \text{K}^{-1}$ for temperatures greater than 362.15 K (89°C), and linearly interpolated between these two values. We have specified a higher thermal conductivity for unconfined SITI experiments that have significant two-phase flow effects. For these unconfined SITI experiments, the thermal conductivity was set to $1.5 \text{ W} \cdot \text{m}^{-1} \text{K}^{-1}$ when temperatures exceeded 445 K (171.85°C).

There are many reaction pathways leading to ignition of Comp-B, however, identifying and parameterizing each reaction is beyond the scope of the current work. Instead, we assume the a single exothermic reaction ($h_{rxn} = -5.87 \times 10^6 \text{ J} \cdot \text{kg}^{-1}$)



or



The non-Arrhenius reaction rate, $r[\text{s}^{-1}]$, is assumed to have the following form :

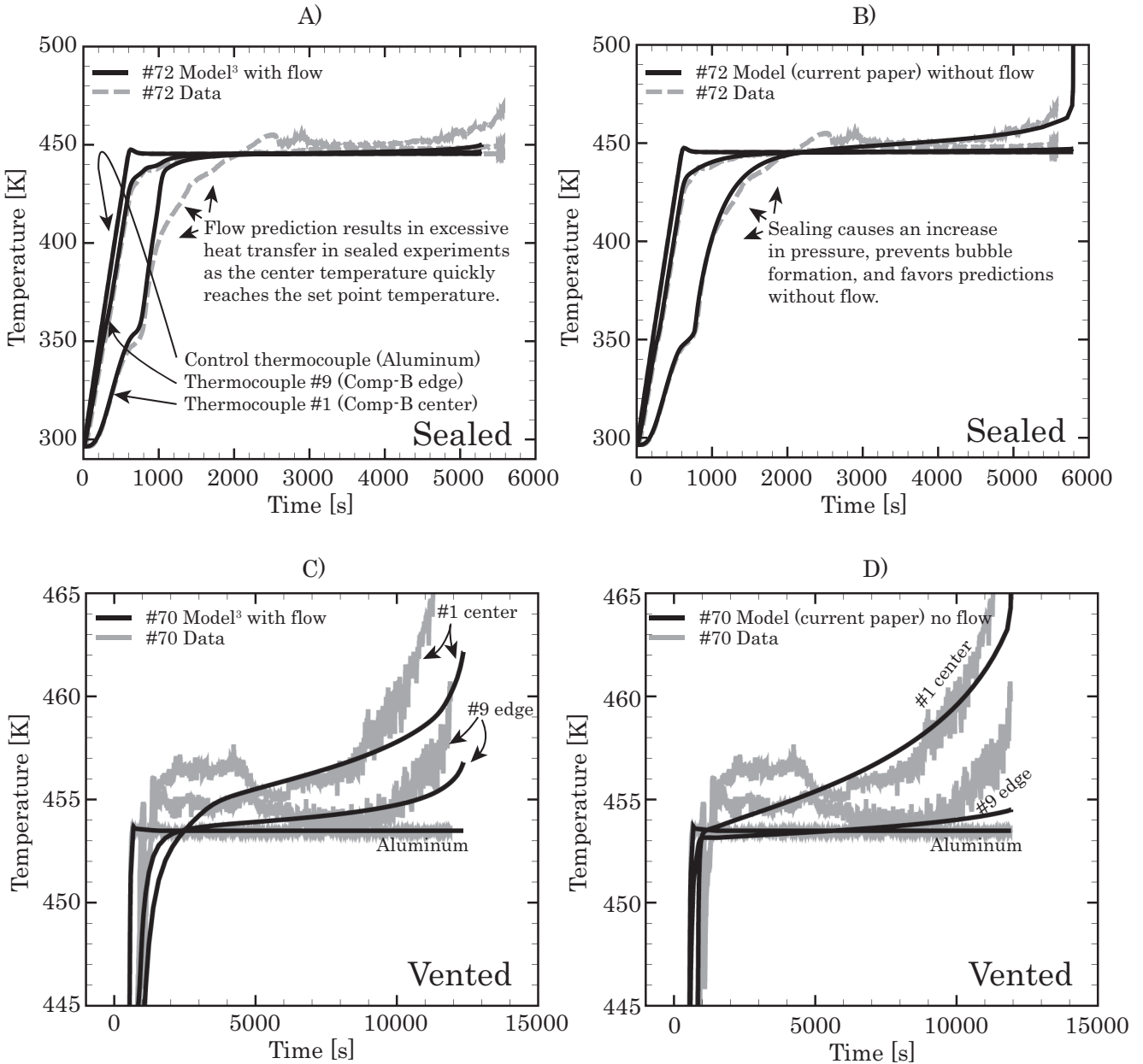


Figure 4 Measured and predicted temperatures from SITI experiment A) #72 using the flow model from reference3, B) #72 without flow model, C) #70 using flow model from reference3, and D) #70 without using flow model.

$$r = A\lambda \exp[-(E + \zeta\sigma_E)/RT][\text{Comp-B}], \quad (4)$$

where A , λ , E/RT , ζ , σ_E/RT , and [Comp-B] are the pre-exponential factor, $\ln A = 30 [\ln (\text{s}^{-1}\text{m}^3 \text{kg}^{-1})]$; liquid rate multiplier; normalized activation energy, 17860 K^{-1} ; distribution parameter, normalized standard deviation of the activation energy, -500 K^{-1} and molar composition of Comp-B [$\text{kmol}\cdot\text{m}^{-3}$]. The liquid rate multiplier, λ , is 1 before RDX melts and 30 after RDX melts. More specifically, the value of λ is 1; while temperature is less than 190°C , increases linearly from 1 to 30 between 190°C and 205°C , and is 30 when the temperature is greater than 205°C . The range of the liquid rate multiplier is slightly different than the melting point range (197.5°C to 207.5°C) discussed earlier in this paper. The acceleration range may be different than the melting range because of RDX dissolution that may also accelerate the rate. We have chosen this range to best match ignition data.

The distributed activation energy model is implemented by using the normsinv function, which is the inverse of the standard normal distribution function. The normsinv function is a standard function in many common spreadsheet programs. The distribution is based on the progress of the reaction, defined as the normalized concentration of Comp-B (e.g. $p = [\text{Comp-B}]/[\text{Comp-B}]_0$); thus, $\zeta = \text{normsinv}(p)$. The negative value of σ_E causes the decomposition reaction to accelerate with the extent of reaction.

In Equation (3), the molecular weight of the Comp-B, gas, and carbon are $100 \text{ g}\cdot\text{mol}^{-1}$, $28 \text{ g}\cdot\text{mol}^{-1}$, and $12 \text{ g}\cdot\text{mol}^{-1}$ respectively. The rate of change of these species can be found from the following equations:

$$\begin{aligned} \frac{d[\text{Comp-B}]}{dt} &= -r, \quad \frac{d[\text{gas}]}{dt} = 3.09r, \\ \text{and } \frac{d[\text{carbon}]}{dt} &= 1.13r. \end{aligned} \quad (5)$$

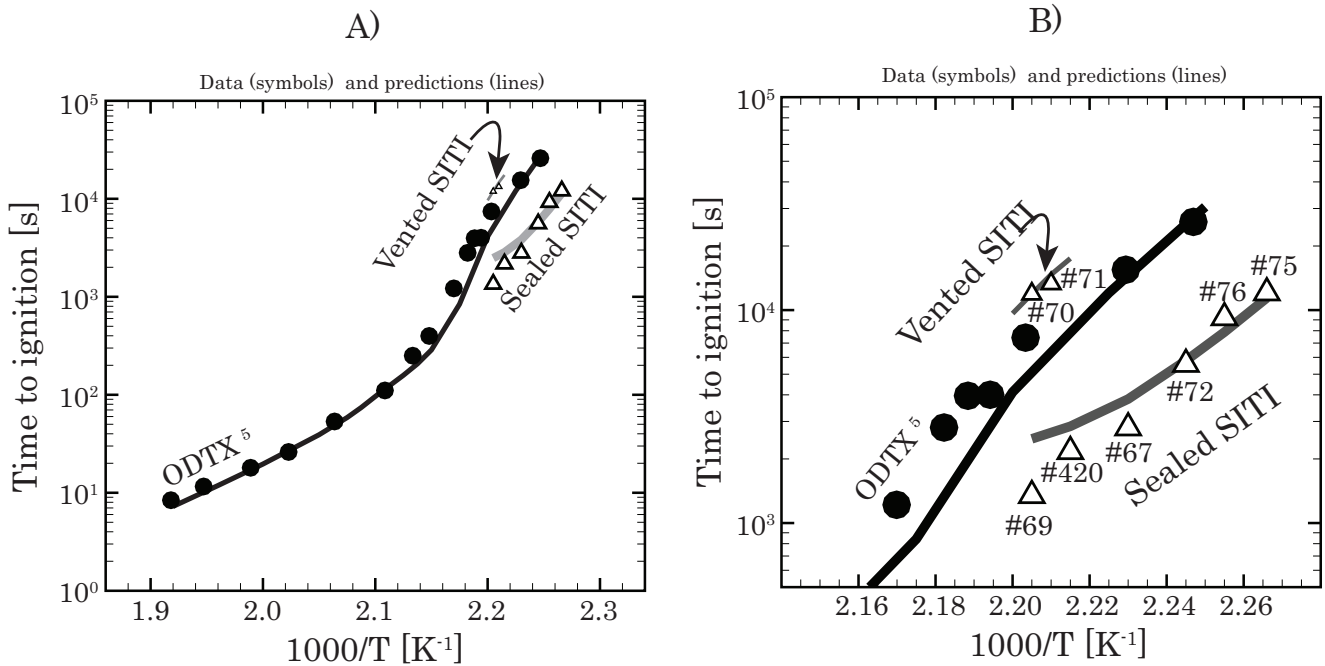


Figure 5 Time to ignition for ODTX,⁵⁾ sealed SITI, and vented SITI. A) Plot emphasizing A) ODTX and B) SITI experiments.

4. Discussion

Figure 4. A shows a simulation of sealed SITI experiment #72 from reference 3 using Boussinesq flow. Figure 4. B shows the same experiment using the model from the current paper without flow. The external aluminum temperature was ramped from room temperature to 172.3°C in about 10 minutes and then the temperature was held at the set point temperature until ignition at 5570 s. The predicted temperatures from the model without flow matches the internal thermocouples better than the model with flow.

Figure 4. C shows a simulation of vented SITI experiment #70 from reference 3 using Boussinesq flow. Figure 4. D shows the same experiment using the model from the current work. The external aluminum temperature was ramped from room temperature to 180.4°C in about 12 minutes and then the temperature was held at the set point temperature until ignition at 11900 s. Despite a higher boundary temperature than #72, the ignition time for #70 was much longer due to the enhanced heat transfer caused by rapid two-phase bubbly flow behavior. Increasing the heat transfer coefficient by a factor of ten mimicked this effect.

Figure 5 shows the measured and predicted ignition times for various ODTX and SITI experiments. Figure 5. A emphasizes the ODTX experiments and Figure 5. B emphasizes the SITI experiments. The boundary condition for the ODTX experiments is a constant temperature boundary condition. This temperature is obtained by heating the aluminum anvils up to a given set point temperature and then at the start of the experiment, hydraulically closing the anvils. These experiments are sealed by deforming a copper gasket around a knife-edge groove near the outer edge of the Comp-B. The pressure inside of the ODTX experiment can get as high as 152×10^6 Pa (22,000 psi), which should inhibit bubble

formation and two-phase flow. The model from the current work without flow matches the experimental ignition times adequately.

Figure 5 also shows both confined and unconfined SITI ignition times. The SITI apparatus is wrapped with heat tape, which is used to ramp the temperature of the external aluminum from ambient conditions to a set point temperature in about 10 minutes; and then, the external aluminum temperature is held at the set point temperature until ignition. The sealed experiments can get up to 14×10^6 Pa (2,000 psi), which also inhibits bubble formation and two phase induced flow. The model is not as good at matching ignition times for the sealed SITI experiments as matching ignition times for the ODTX experiments. Perhaps the lower pressure causes some flow effects, which should be included in future modeling efforts.

Flow effects may become more significant as pressure decreases. The vented SITI experiment does not inhibit bubble formation and the thermally degraded Comp-B becomes well stirred. In the limit, this might be modeled as a zero-dimensional single temperature material or as material with a high thermal conductivity at temperatures where flow is expected to be vigorous. In the current work, we chose to increase the thermal conductivity of the Comp-B by a factor of 10 when temperatures exceed 167°C to mimic the increased heat transfer due to the bubbly flow.

5. Conclusions

Previous researchers,^{2,4)} including our laboratory,³⁾ have concluded that flow plays a major role in the cookoff of Comp-B, which is a melt-castable explosive. However, we have shown in the current work that flow plays a *minor role in sealed experiments* such as the ODTX experiments where pressures can get as high as 152×10^6

Pa. We have also shown pictures in both a sealed and a vented cookoff experiment showing bubble formation being inhibited as pressure increases. When the experiments are vented, bubble formation causes rapid bubble-induced flow resulting in increased heat transfer and delayed ignition.

5. Acknowledgements

Sandia National Laboratories is a multiprogram laboratory operated by Sandia Corporation, a Lockheed Martin Company, for the U.S. Department of Energy's National Nuclear Security Administration under Contract DE-AC04-94AL85000. Internal document number is SAND 2014-19216 J. The authors acknowledge the Joint DoD/DOE Munitions Program for partial support of this work. We would like to thank Shane Snedigar (SNL) for running the SITI experiments, Dave Zerkle at Los Alamos National Laboratory (LANL) for many discussions regarding cookoff and viscosity of Comp-B, Mel Baer

(SNL) for discussions regarding decomposition of melt-castable explosives, Bill Erikson (SNL) and Mark Anderson (SNL) for internal review, and Clint Hall, Anthony Geller, Leanna Minier for management support.

6. References

- 1) V. Fung, M. Ervin, B. Alexander, C. Patel, and P. Samuels, Proc. 2010 Insensitive Munitions and Energetic Materials Technology Symposium, Munich, Germany (2010).
- 2) D. K. Zerkle, Proc. Thirteenth International Detonation Symposium, 771–777, Norfolk, (2006).
- 3) M. L. Hobbs, M. J. Kaneshige, and M. U. Anderson, JANNAF 27th Propulsion Systems Hazards Joint Subcommittee Meeting, Monterey, (2012).
- 4) M. A. McClelland, E. A. Glascoe, A. L. Nichols, S. P. Schofield, and H. K. Springer, Proc. Fifteenth International Detonation Symposium, San Francisco, (2014).
- 5) R. R. McGuire and C. M. Tarver, Proc. Seventh Symposium (International) on Detonation, 56–64, Annapolis, (1981).